Estimation of nearshore water depth using physics-informed deep learning

Nan Wang

Department of Civil and Environmental Engineering, Northeastern University, 400 SN, Boston, MA 02115
wang.nan@northeastern.edu

Qin Chen

Department of Civil and Environmental Engineering, Northeastern University, 471 SN, Boston, MA 02115
q.chen@northeastern.edu

This paper develops physics-informed neural networks (PINNs) to estimate water depths from remote sensing of the nearshore. The model integrates the knowledge of water wave mechanics and fully connected neural networks to determine the water depth and reconstruct the surface wave field. Two test cases were used to assess the performance of PINNs for solving depth inversion problems, including linear waves over a three-dimensional (3D) barred beach and nonlinear waves over an alongshore uniform beach. The results show that the developed PINN model is able to estimate the 3D nearshore bathymetry with sufficient accuracy. It is found that one of the advantages of using PINNs to solve bathymetry inversion problems is that the nonlinear dispersion relation of water waves can be embedded in the model. Thus, the effect of amplitude dispersion on depth inversion and wave field prediction can be taken into account. Overall, our results show that the inverse PINN model is a promising tool for estimating nearshore bathymetry based on observations from various remote sensing platforms.

Keywords: Physics-informed neural networks, Depth inversion, Wave field reconstruction, Nearshore wave processes

1 INTRODUCTION

Due to increasing coastal utilization and sea level rise, accurate information about the nearshore bathymetry is essential for designing and operating many coastal projects, such as flood protection and coastal zone management. In general, it can be costly to collect nearshore bathymetric data using in-situ methods, such as vessel-based and bottom contact survey techniques, which become impartial due to the hazardous surf zone conditions during storms. Even when the in-situ measurements are available, the spatial undersampling may not well resolve complex bathymetric features, and temporal undersampling may also poorly capture beach changes in the highly dynamic environment. Therefore, it would be desirable to monitor the nearshore regions using remote sensing techniques, which can have a broader spatial and temporal coverage than the traditional in-situ surveying methods do [1].

In the past several decades, many studies have focused on solving the bathymetric inversion problems using observed surface wave properties and simple physical models. For example, cBathy is a popular bathymetric inversion algorithm that uses the linear wave dispersion relationship to estimate the nearshore bathymetry with wave celerity obtained from remote sensing techniques and a Kalman filtered update framework [2]. The algorithm was found to deteriorate during storms when waves transition from non-breaking to breaking in the surf zone [3]. Another popular bathymetry inversion

technique is data assimilation, which combines observational data and dynamical systems to generate a state estimation while accounting for uncertainty in the observations and model dynamics [4]. Data assimilation tries to minimize a cost function based on the difference between observations and simulations with an initial estimate of the unknown parameters and uncertainties to regularize the solution [5]. Wilson et al. (2014) estimated bathymetry as an uncertain parameter in a data assimilation system with the ensemble Kalman filter based on time-dependent remote sensing observations. The results show that the bathymetry can be estimated with good accuracy, and nearshore forecasts can be improved by assimilating remotely sensed data.

Recently, the development of machine learning (ML) methods, hardware resources, and sensing technologies have created new opportunities for using soft computing-based models to explore nearshore bathymetry [6]. Unlike the data assimilation method, soft-computing models do not require simulations from deterministic forward numerical models or knowledge about the uncertainty of observations and the uncertainty of the numerical model. Using the data assimilation method to solve the inverse problem can be computationally expensive, since it may require thousands or millions of forward model simulations for evaluating estimators and characterizing posterior distributions of parameters [7]. Thus, applying ML to obtain the solution of inverse problems would be desirable because it can execute faster. Recently, using PINNs (physics-informed neural networks) to solve inverse problems has been the focus of many studies, because the addition of physics-based loss terms can generate more accurate and robust results [7]. For example, Raissi et al. (2019) predicted the lift and drag forces of a system based on sparse data of the velocity field with physics-guided loss functions. Also, Kahana et al. (2020) used a neural network with a physically informed loss component to identify the location of an underwater obstacle, showing that the PINN approach can generalize well and produce promising results.

The purpose of this study is to develop an inverse model for estimating nearshore bathymetry based on physics-informed deep learning of remote sensing data (i.e., wave number and significant wave height) with PINNs. The feasibility of reconstructing wave fields and inferring water depths in shallow waters with scarce wave measurements was investigated.

2 METHODOLOGY

This study focuses on developing accurate inverse PINN models to estimate nearshore bathymetry with post-processed geophysical parameters from remote sensing platforms, such as X-band marine radar or stereo-photogrammetry, including wave heights and wave numbers. It is worth mentioning that the main purpose of this work is not to extract quantitative hydrodynamic information from surf zone imagery. Thus, the digital image processing of remote sensing data is not covered in this study. Moreover, it is assumed that the parameters derived from the remote sensing platforms are sufficiently accurate in this work. Two test scenarios were employed to assess the performance of PINNs for solving the depth inversion problems, which are linear waves over a 3D barred beach and nonlinear waves over an alongshore uniform barred beach.

2.1 Energy balance equation for wave propagation in shallow waters

In this study, we developed a novel composite PINN model to solve the depth inversion problem and reconstruct wave fields in the nearshore area. Wave shoaling, refraction, and depth-limited breaking were considered in this model. The governing equations encoded into the fully connected neural networks include the wave energy balance equation and dispersion relation. The effects of amplitude dispersion (i.e., nonlinear dispersion relation) on depth inversion and wave field prediction were also investigated. This study focuses on stationary wave fields without wind forcing and ambient currents. For water waves, the energy balance equation is given by

$$\frac{\partial ec_{gx}}{\partial x}+\frac{\partial ec_{gy}}{\partial y}+\frac{\partial ec_{g\theta}}{\partial \theta}+d_w=0 \tag{1}$$

where e is the wave energy density in each directional bin, c_g is the group velocity, θ represents the angle of incidence with respect to the *x*-axis, and d_w is the dissipation of energy density caused by wave breaking [10]. The Janssen and Battjes (2007) formulation for wave breaking was applied in this work. The total wave dissipation was distributed proportionally over the wave directions using the following formulation

$$d_w(x,y,\theta)=\frac{e(x,y,\theta)}{E(x,y)}\overline{D}_w(x,y) \tag{2}$$

where $\overline{D}_w$ denotes the expected value of the power dissipated per unit area. The root-mean-square wave height was calculated based on $H_{\mathrm{rms}}=\sqrt{\frac{8E}{\rho g}}$, and $E=\int_0^{2\pi}e(\theta)d\theta$. For unidirectional waves, the wave energy balance equation over an alongshore uniform beach becomes $\frac{\partial Ec_{gx}}{\partial x}+\overline{D}_w=0$.

2.2 Physics-informed neural networks

By infusing the governing equations into the artificial neural networks, PINNs can bridge the gap between ML-based methods and scientific computations and deduce solutions involving partial differential equations. To solve the depth inversion problems over a 3D beach with the linear dispersion relation, the corresponding residuals were defined as

$$f_1(x,y,\theta):=\frac{\partial ec_{gx}}{\partial x}+\frac{\partial ec_{gy}}{\partial y}+\frac{\partial ec_{g\theta}}{\partial \theta}+d_w \tag{3}$$

$$f_2(x,y):=\omega^2-gk\tanh(kd) \tag{4}$$

where h represents the local water depth, k is the wave number, and ω is the angular frequency. To consider the effects of amplitude dispersion on depth inversion [12] and wave field prediction for nonlinear waves over an alongshore uniform beach, the residuals were determined as

$$f_1(x):=\frac{\partial Ec_{gx}}{\partial x}+\overline{D}_w \tag{5}$$

$$f_2(x):=\omega^2-gk(1+\mathcal{F}_1(kd)\epsilon^2 D)\tanh\left(kd+\mathcal{F}_2(kd)\epsilon\right) \tag{6}$$

where $D=\frac{\cosh(4kd)+8-2\tanh^2(kd)}{8\sinh^4(kd)}$, $\mathcal{F}_1(kd)=\tanh^5(kd)$, $\mathcal{F}_2(kd)=\left[\frac{kd}{\sinh(kd)}\right]^4$, $\epsilon=k|A|$, and $|A|=1/2H_{rms}$. These residuals were used as restraints during the training of PINNs to generate physically consistent predictions. Additionally, the wave measurements scattered in the computational domain were also used to constrain the model, such as wave height, wave angle, and wave number. The schematic representation of the algorithm for solving depth inversion problems is shown in Figure 1. The loss function consists of two main parts. The first part corresponds to the collocation points (i.e., residual loss), where the physical constraints were imposed to encourage Eqn (3) and (4) (or Eqn (5) and (6)) to equal zero. The second part encouraged the outputs of PINNs to match wave parameters obtained from field observations (using the outputs of the physics-based nearshore model XBeach [13] in this study for PINNs testing). Therefore, the total loss function for solving the depth inversion problem of linear waves is given as

$$\begin{aligned}\mathcal{L}_{total}&=\mathcal{L}_{residual}+\mathcal{L}_{measurements}\\&=\mathcal{L}_{f_1}+\lambda_{f_2}\times\mathcal{L}_{f_2}+\lambda_{H_{\mathrm{rms}}}\times\mathcal{L}_{H_{\mathrm{rms}}}+\lambda_{\theta_{\mathrm{m}}}\times\mathcal{L}_{\theta_{\mathrm{m}}}+\lambda_k\times\mathcal{L}_k\end{aligned} \tag{7}$$

where λ_{f_2}, $\lambda_{H_{\mathrm{rms}}}$, $\lambda_{\theta_{\mathrm{m}}}$, and λ_k are the weighting coefficients for balancing the interplay between different terms in the loss function [14]. Hyperbolic tangent was used in this study as the activation function, and the networks were initialized with

Xavier initialization. The network structure was kept identical to four hidden layers of 30 nodes for each test case. In this study, the training was implemented on an NVIDIA v100-sxm2 GPU with the TensorFlow platform.

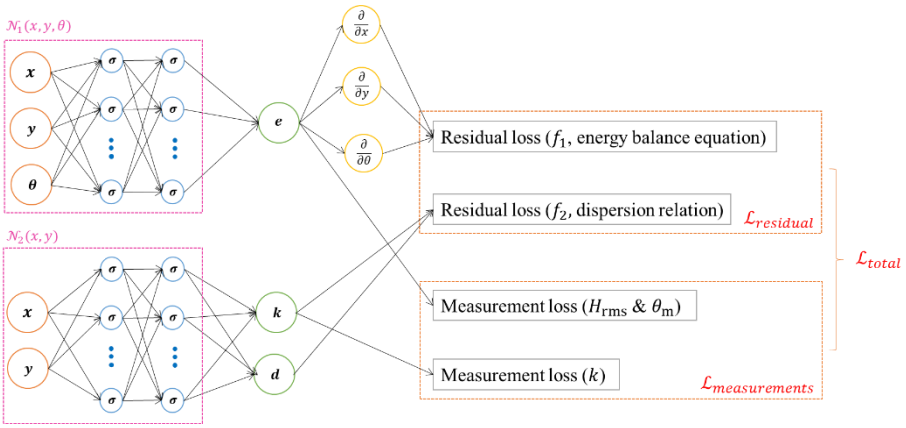

Figure 1. A schematic representation of the proposed algorithm for solving the depth inversion problems.

2.2.1Three-dimensional barred beach.

The wave condition offshore of the 3D barred beach was set as H_{rms} = 1 m and peak wave period (T_{p}) = 8 s. The incident wave angle follows the directional distribution of $\cos^{\mathrm{m}}(\theta - \theta_{\mathrm{m}})$ with $\theta_{\mathrm{m}} = -30^{\circ}$ and $\mathrm{m} = 20$. Numerical simulations of H_{rms} and θ_{m} from XBeach were employed as training and testing data. The resolution of directional spreading of waves ($d\theta$) was set to 10° in both XBeach and PINN models, and the lower and upper directional limits were defined as -90° to 90°, respectively. It was assumed that the wave number and wave angle were known at every location, meaning that the wave number and wave angle over the entire study area were used as training data for the model. The training data for H_{rms} were set at the locations listed in Table 1. Specifically, we randomly selected a total of 100 training points over the entire domain. Fifteen of them are in the offshore domain. Thirty-five are in the shoaling zone. The rest of the 50 points are in the surf zone. The total number of training points is about 2% of the entire computational data. To get a better accuracy, more training points were selected in the shoaling and breaking zones since strong wave height variations happen in these two areas. In reality, we do not know where is the shoaling zone and breaking zone since the bathymetry is unknown. Thus, it was assumed that the breaking zone is from 800 m to 980 m, and more training points were set in this region. A total of 4653 collocation points were uniformly distributed from x = 0-980 m and y = 20-480 m to constrain learning for generating physically consistent predictions.

Table 1. The locations of training points of H_{rms} for reconstructing wave fields over the alongshore uniform barred beach.

Location	x = 0-500 m	x = 500-800 m	x = 800-980 m
# training points	15	35	50

Adam (adaptive moment estimation) and L-BFGS-B (limited memory Broyden–Fletcher–Goldfarb–Shanno with boundaries) were used as network training functions [15]. The Adam optimizer was employed to produce a better set of initial neural network variables, and L-BFGS-B was used to further fine-tune the PINN networks to minimize test errors [14]. The initial learning rate of Adam was set to 10^{-4} and then decreased to 80% of the previous rate every 5000 iterations. 8×10^{4} Adam iterations were implemented before the L-BFGS-B training, which was then automatically terminated based

on the increment tolerance. The error statistics were computed to quantify the prediction skills of PINNs, including root mean square error (*RMSE*) and coefficient of discrimination (R^2).

2.2.2 An alongshore uniform barred beach

Compared to cBathy, one advantage of utilizing PINNs to solve the bathymetry inversion problem is that nonlinear dispersion relation could be embedded in the model. cBathy inverts the linear wave dispersion relationship to estimate the nearshore bathymetry. The estimation accuracy of cBathy decreases with an increase in wave height due to the omission of amplitude dispersion of nonlinear waves [5]. To test the PINNs' ability to account for the effect of wave nonlinearity in the nearshore, we used the nonlinear dispersion relation instead of the linear dispersion relation to reconstruct the wave field and estimate the bathymetry over an alongshore uniform barred beach with known wave numbers. The wave boundary condition of the nonlinear waves was set as $H_{rms} = 1$ m, $T_p = 8$ s, and the incident wave angle of 30˚. The wave height training data was set at x = 100 m, and wave numbers were known every 4 m from x = 0 -1000 m. Similar to the PINN model for estimating the water depth of a 3D barred beach, Adam and L-BFGS-B were used as network training functions, with 4×10^4 Adam iterations conducted before L-BFGS-B started. To examine the prediction performance of the model for reconstructing the wave field, the outputs of H_{rms} were compared to the numerical solutions to the wave energy balance equation.

3 RESULTS

3.1 Water waves over a 3D barred beach

In this section, the outputs from XBeach and PINNs were compared to investigate the feasibility of using PINNs to estimate water depth and reconstruct wave fields over a 3D barred beach. The red dots in Figure 2 (a) present the locations of H_{rms} training points. The 3D plot shows the simulated spatial variation of H_{rms} by PINNs, which is in good agreement with the numerical results from XBeach. The contour plot in Figure 2 (b) depicts the difference between the PINN simulation and true bathymetry. It can be observed that PINNs have good prediction skills for estimating the water depths with small errors (*RMSE* = 0.014 m). Also, comparisons of the simulation outputs from the PINNs and XBeach are shown in Figure 2 (c), indicating that the PINN-predicted H_{rms} and θ_{m} correlated well with those from XBeach. Overall, the developed PINN model shows a promising ability to estimate water depths and reconstruct wave fields over a 3D barred beach.

3.2 Effects of amplitude dispersion on depth inversion and wave field prediction

Figure 3 (a) shows that the PINN outputs correlate well with the numerical solution to the energy balance equation (RMSE values are 0.001 m and 0.019 m for estimating H_rms and d, respectively) with the nonlinear dispersion relation embedded in the model. It can be observed that the simulation skills of the PINN model with the linear dispersion relation deteriorate in the surf zone (Figure 3 (b)), suggesting that the linear PINN model has a similar pattern as cBathy. In other words, the PINNs embedded with the linear dispersion relation are not capable of learning the effect of nonlinear waves on the dispersion relation. This finding indicates that selecting an appropriate physical constrain is crucial for solving the depth inverse problems and reconstructing wave fields with sufficient accuracy.

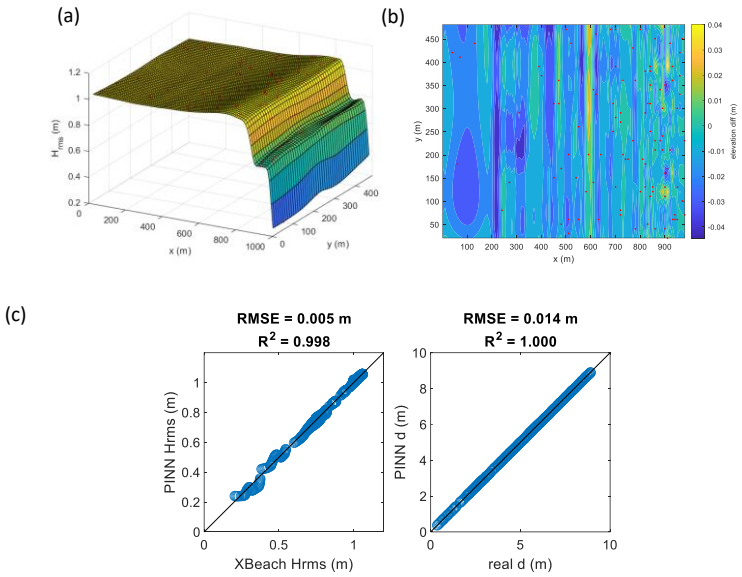

Figure 2. Comparison between the XBeach and PINN outputs over the 3D barred beach. (a) spatial variation of the PINN-predicted wave fields. The red dots represent the location of training points; (b) the contour figure shows the difference between the PINN-predicted depth and real bathymetry; (c) scatter plots of the predicted H_{rms} and d. The plots only contain testing data.

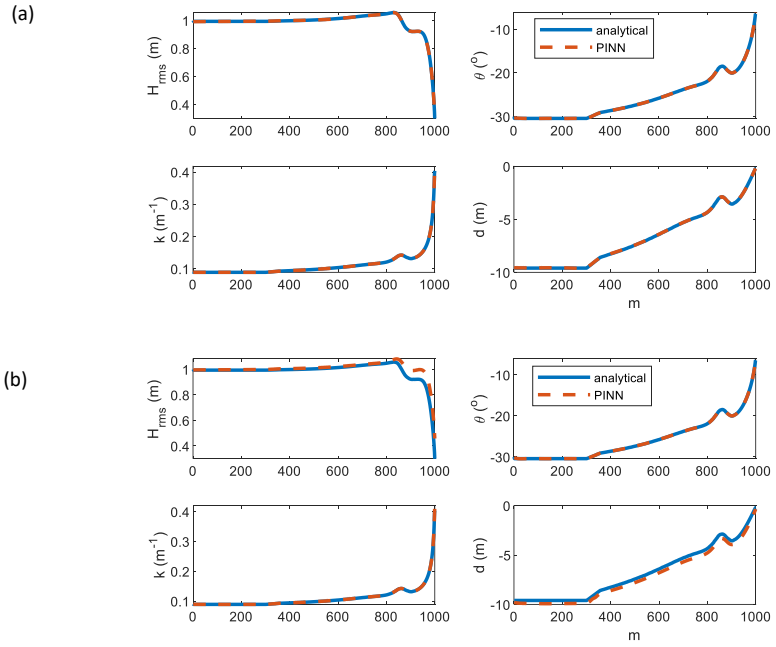

Figure 3. Comparisons between analytical and PINN-simulated H_{rms}, wave angle, wave number, and water depth with (a) nonlinear dispersion relation and (b) linear dispersion relation.

4 DISCUSSION

The sensitivity of the performance of PINNs to the number and distribution of training points of H_{rms} is investigated in this section. Because strong variations of wave height happen in the surf zone where wave breaking dissipates wave energy, we use different numbers of training points at x = 500-980 m. Unsurprisingly, the results indicate that the *RMSE* of H_{rms} decreases when the number of training points increases (Table 2). Furthermore, if the total number of training points is fixed, a higher accuracy (i.e., mean error of H_{rms}) could be obtained when more training points were placed close to the shore from x = 800-980 m. This can be explained by the fact that the gradient of wave height variation is higher due to the depth-limited wave breaking. Since the wave number was assumed to be known at every point inside the computational domain, the accuracy of the estimated bathymetry is very good. It is worth mentioning that the model does not require the wave number at every location as training points (Section 3.2).

Table 2. Error statistics of the simulated H_{rms}, θ_m, and d over the 3D barred beach with different training points of H_{rms} applied in PINNs.

	RMSE		R^2		Max error	
	H_{rms} (m)	d (cm)	H_{rms}	d	H_{rms} (m)	d (cm)
o15n35o50[a]	0.005	1.450	0.998	1.000	0.171	1.63
o15n35o40	0.006	1.460	0.998	1.000	0.155	1.59
o15n35o30	0.017	1.520	0.984	1.000	0.409	1.72
o15n35o20	0.016	1.470	0.989	1.000	0.474	2.02
o15n35o10	0.032	1.460	0.979	1.000	0.452	2.24
o15n30o50	0.008	1.450	0.997	1.000	0.369	1.91
o15n20o50	0.008	1.450	0.996	1.000	0.350	1.91
o15n10o50	0.010	1.470	0.995	1.000	0.388	1.93

[a]o15n35o50 means 15, 35, and 50 training points were set at x = 0-500 m, 500-800 m, and 800-980 m, respectively.

5 SUMMARY AND CONCLUSIONS

In this study, we developed an inverse PINN model to estimate nearshore bathymetry based on remote sensing data (i.e., wave number and significant wave height) by combining the prior knowledge of wave mechanics into the fully-connected neural networks. The feasibility of reconstructing a wave field and estimating the water depth in shallow waters with limited field observations was investigated. Assuming surface wave celerity (or wave number) and wave height measurements are available from various remote sensing platforms, two test scenarios were used to assess the performance of PINNs for solving depth inversion problems, including linear waves over a 3D barred beach and nonlinear waves over an alongshore uniform barred beach. The results show that the developed PINN model is able to estimate 3D nearshore bathymetry with sufficient accuracy. The spatial distribution of wave height can also be predicted with high resolution. Furthermore, the sensitivity of PINNs to the number and location of training points of H_{rms} was investigated. It was found that the *RMSE* of H_{rms} decreases when the number of training points increases. Moreover, if the total number of training points is fixed, higher accuracy can be obtained when more training points are placed in the surf zone. In contrast, the model performance for predicting bathymetry is less sensitive to the locations of training points of H_{rms}.

One advantage of applying PINNs to solve bathymetry inversion problems is that the effect of wave nonlinearity can be embedded in the model. In this study, we used the nonlinear dispersion relation instead of the linear dispersion relation together with the energy balance equation as the physical laws to reconstruct the wave field and estimate the bathymetry over an alongshore uniform barred beach with known wave numbers. The results show that the PINN outputs correlate well with the direct numerical solution to the energy balance equation (*RMSE* values are 0.001 m and 0.019 m for estimating the wave height and water depth, respectively).

This study is the first attempt to investigate the capability of PINNs for estimating nearshore bathymetry and reconstructing wave fields with limited field observations. Though the current results are encouraging, open questions remain. For example, are PINNs able to infer the bottom friction coefficient or wave breaking parameters dynamically? Is it practical to use PINNs to solve depth inversion problems and reconstruct wave fields under storm conditions? What are the potential errors of PINNs when remotely sensed data are inaccurate and the embedded physics are incomplete? More studies will be carried out to answer those questions and to further test the performance of PINNs under field conditions.

ACKNOWLEDGMENTS

Funding for the study has been provided by the U.S. National Science Foundation (NSF Grants 1856359 and 2139882).

REFERENCES

[1] G. W. Wilson, H. T. Özkan-Haller, R. A. Holman, M. C. Haller, D. A. Honegger, and C. C. Chickadel, "Surf zone bathymetry and circulation predictions via data assimilation of remote sensing observations," *J. Geophys. Res. Ocean.*, vol. 119, no. 3, pp. 1993–2016, 2014.

[2] R. Holman, N. Plant, and T. Holland, "cBathy: A robust algorithm for estimating nearshore bathymetry," *J. Geophys. Res. Ocean.*, vol. 118, no. 5, pp. 2595–2609, 2013.

[3] D. A. Honegger, M. C. Haller, and R. A. Holman, "High-resolution bathymetry estimates via X-band marine radar: 1. beaches," *Coast. Eng.*, vol. 149, pp. 39–48, 2019.

[4] J. M. Lewis, S. Lakshmivarahan, and S. Dhall, *Dynamic data assimilation: a least squares approach*, vol. 13. Cambridge University Press, 2006.

[5] A. Salim and G. Wilson, "Validation and analysis of a 1-D variational assimilation scheme for bathymetry inversion," *Coast. Eng.*, vol. 167, p. 103895, 2021.

[6] A. Eldesokey, M. Felsberg, and F. S. Khan, "Confidence propagation through cnns for guided sparse depth regression," *IEEE Trans. Pattern Anal. Mach. Intell.*, vol. 42, no. 10, pp. 2423–2436, 2019.

[7] J. Willard, X. Jia, S. Xu, M. Steinbach, and V. Kumar, "Integrating physics-based modeling with machine learning: A survey," *arXiv Prepr. arXiv2003.04919*, 2020.

[8] M. Raissi, Z. Wang, M. S. Triantafyllou, and G. E. Karniadakis, "Deep learning of vortex-induced vibrations," *J. Fluid Mech.*, vol. 861, pp. 119–137, 2019.

[9] A. Kahana, E. Turkel, S. Dekel, and D. Givoli, "Obstacle segmentation based on the wave equation and deep learning," *J. Comput. Phys.*, vol. 413, p. 109458, 2020.

[10] L. H. Holthuijsen, N. Booij, and T. H. C. Herbers, "A prediction model for stationary, short-crested waves in shallow water with ambient currents," *Coast. Eng.*, vol. 13, no. 1, pp. 23–54, 1989.

[11] T. T. Janssen and J. A. Battjes, "A note on wave energy dissipation over steep beaches," *Coast. Eng.*, vol. 54, no. 9, pp. 711–716, 2007.

[12] J. T. Kirby and R. A. Dalrymple, "An approximate model for nonlinear dispersion in monochromatic wave propagation models," *Coast. Eng.*, vol. 9, no. 6, pp. 545–561, 1986.

[13] D. Roelvink, A. Reniers, A. P. Van Dongeren, J. V. T. De Vries, R. McCall, and J. Lescinski, "Modelling storm impacts on beaches, dunes and barrier islands," *Coast. Eng.*, vol. 56, no. 11–12, pp. 1133–1152, 2009.

[14] X. Jin, S. Cai, H. Li, and G. E. Karniadakis, "NSFnets (Navier-Stokes flow nets): Physics-informed neural networks for the incompressible Navier-Stokes equations," *J. Comput. Phys.*, vol. 426, p. 109951, 2021.

[15] D. P. Kingma and J. Ba, "Adam: A method for stochastic optimization," *arXiv Prepr. arXiv1412.6980*, 2014.